Tryptophan to phenylalanine substitutions allow differentiation of short- and long-range conformational changes during denaturation of goat α-lactalbumin

ARTICLE *in* PROTEINS STRUCTURE FUNCTION AND BIOINFORMATICS · JULY 2005

Impact Factor: 2.63 · DOI: 10.1002/prot.20496 · Source: PubMed

7 AUTHORS, INCLUDING:

Zsuzsa Majer
Eötvös Loránd University
118 PUBLICATIONS **1,226** CITATIONS
SEE PROFILE

Marcel Joniau
University of Leuven
87 PUBLICATIONS **1,679** CITATIONS
SEE PROFILE

Herman Van Dael
University of Leuven
46 PUBLICATIONS **881** CITATIONS
SEE PROFILE

Tryptophan to Phenylalanine Substitutions Allow Differentiation of Short- and Long-Range Conformational Changes during Denaturation of Goat α-Lactalbumin

Ann Vanhooren,[1] Allel Chedad,[1] Viktor Farkas,[2] Zsuzsa Majer,[2] Marcel Joniau,[1] Herman Van Dael,[1] and Ignace Hanssens[1]*

[1]*Interdisciplinary Research Center, Katholieke Universiteit Leuven Campus Kortrijk, Kortrijk, Belgium*
[2]*Department of Organic Chemistry, Eötvös Loránd University, Budapest, Hungary*

ABSTRACT **To test the occurrence of local particularities during the unfolding of Ca^{2+}-loaded goat α-lactalbumin (GLA) we replaced Trp60 and -118, either one or both, by Phe. In contrast with alternative studies, our recombinant α-lactalbumins are expressed in *Pichia pastoris* and do not contain the extra N-terminal methionine. The substitution of Trp60 leads to a reduction of the global stability. The effect of the Trp118Phe substitution on the conformation and stability of the mutant, however, is negligible. Comparison of the fluorescence spectra of these mutants makes clear that Trp60 and -118 are strongly quenched in the native state. They both contribute to the quenching of Trp26 and -104 emission. By the interplay of these quenching effects, the fluorescence intensity changes upon thermal unfolding of the mutants behave very differently. This is the reason for a discrepancy of the apparent transition temperatures derived from the shift of the emission maxima ($T_{m,\mathrm{Fl}\ \lambda}$) and those derived from DSC ($T_{m,\mathrm{DSC}}$). However, the transition temperatures derived from fluorescence intensity ($T_{m,\mathrm{Fl\ int}}$) and from DSC ($T_{m,\mathrm{DSC}}$), respectively, are quite similar, and thus, no local rearrangements are observed upon heat-induced unfolding. At room temperature, the occurrence of specific local rearrangements upon GdnHCl-induced denaturation of the different mutants is deduced from the apparent free energies of their transition state obtained from stopped-flow fluorescence measurements. By $\phi^{\ddagger}$-value analysis it appears that, while the surroundings of Trp118 are exposed in the kinetic transition state, the surroundings of Trp60 remain native. Proteins 2005; 60:118–130.** © 2005 Wiley-Liss, Inc.

Key words: Trp-Phe mutants; protein folding; thermal unfolding; chemical unfolding; circular dichroism; fluorescence; stopped-flow kinetics; differential scanning calorimetry

INTRODUCTION

α-Lactalbumin (LA) performs an important function in mammary secretory cells as it acts as a regulatory subunit of the lactose synthase system.[1] In complex with galactosyltranferase, LA modifies the specificity of the enzyme so that it can catalyze the transfer of galactose to glucose.[2] Most LAs, including human, bovine, and goat LA, consist of 123 amino acid residues. X-ray crystallographic analysis has shown that the three-dimensional structure of LA is very similar to that of c-type lysozymes.[3] Although the native proteins are compact, their structure consists of two clearly distinct parts: an α- and a β-domain. The two domains are divided by a deep cleft, which, in the homologeous lysozyme, represents the substrate binding site. Ca^{2+} ions bind to all LAs and stabilize the protein against denaturation.[4] The Ca^{2+}-binding loop connects both domains and is absent in most lysozymes.[3,5]

LA exhibits a partially unfolded state, the molten globule, which is stably populated at equilibrium under various mildly denaturing conditions.[6,7] The molten globule conformer is characterized by a native-like α-domain, while the β-domain (residues 35–85) is largely unstructured.[8] The similarity of the LA molten globule conformer to an early intermediate on the folding pathway has led to extensive study of LA as a model for protein folding.[9,10] Other conformers that are intermediate between the native and the molten globule state also have been reported.[11,12] An aggregated, misfolded form of LA causes apoptosis in tumor but not in normal cells,[13] indicating that some of the partially folded states of LA may be biologically important.

Besides the major part of the β-domain, also the sequences 105–110 and 112–119 at the surface of the α-helical domain are characterized by high flexibility and conformational variability.[14] The side chains of Gln117 and

Abbreviations: LA: α-lactalbumin, BLA: bovine α-lactalbumin, GLA: goat α-lactalbumin, MES: (2-(N-morpholino)ethanesulfonic acid), Tris-HCl: buffer of tris(hydroxymethyl)aminomethane pH adjusted with hydrochoride, GdnHCl: guanidine hydrochloride. $T_{m,\mathrm{DSC}}$, $T_{m,Fl\ \lambda}$ and $T_{m,Fl\ int}$ are the midpoint temperatures of the transition curves upon thermal unfolding of GLA as measured from heat capacity changes, from the shift of the emission maximum and from the fluorescence intensity, respectively.

Grant sponsor: the Flemish Fund for Scientific Research; Grant number: G-0180-03; Grant sponsor: the Hungarian Scientific Research Foundation; Grant number: OTKA T 037719.

*Correspondence to: Ignace Hanssens, Interdisciplinary Research Center, Katholieke Universiteit Leuven Campus Kortrijk, B-8500 Kortrijk, Belgium. E-mail: ignace.hanssens@kulak.ac.be

Received 31 August 2004; Accepted 30 January 2005

Published online 28 April 2005 in Wiley InterScience (www.interscience.wiley.com). DOI: 10.1002/prot.20496

Fig. 1. Crystal structure of goat LA generated from coordinates deposited in the Brookhaven Protein Data Bank, HFY,[14] using the program SWISS-MODEL.[59] The side chains of the four Trp residues are represented by sticks.

Trp118 are essential for efficient binding with galactosyltransferase.[15–17] The vicinal sequence 105–110, although itself not in contact with the enzyme, is also important for the formation of the lactose synthase complex.[17,18] This flexible region adopts either a loop or a helix conformation, depending on the pH of the medium.[14] Ramakrishnan et al.[19,20] showed that, in mouse LA, this region adopts a helical conformation when bound in the lactose synthase complex.

In the present study we replaced Trp60 and Trp118 in goat LA, either one or both, by Phe. As mentioned above, Trp60, as well as Trp118, are surrounded by flexible sequences. Both sequences are, however, located in different regions. Figure 1 represents the structure of GLA and indicates the sites of mutation. Trp60 is located in the β-domain, near the cleft region. Trp118 is located near the C-terminus, in a flexible region of the α-domain. This study aims to obtain information on local aspects of organization and of destabilization within the LA molecule. This is accessed by comparing the spectral characteristics deduced from emission fluorescence and from near-UV CD spectroscopy with the DSC scans of the various mutants.

Emission fluorescence and near-UV CD spectroscopy are two commonly used techniques for the observation of conformational changes in proteins. Both techniques make use of Trp as a reporter and are very sensitive to the local environment of the Trp groups.[21,22] As LAs generally have four Trp residues, the observed fluorescence and CD signals are a superposition of the individual signals. To study the proper contribution of a specific Trp, the other Trp groups can be substituted with nonfluorescent amino acids as was done by Chakraborty et al. for human LA.[23] We, on the other hand, followed an alternative way in which we substituted a single Trp with a nonfluorescent amino acid, and from the difference spectrum of the mutant with respect to the wild-type protein, we deduced the specific contribution of the substituted Trp. Such single-point mutations minimize the direct disturbance of protein biophysical properties such as stability, flexibility, and folding kinetics. We measured fluorescence to follow thermal as well as GdnHCl-induced unfolding. The fluorescence data of wild-type and mutant GLA were compared to detect local effects on the stability, kinetics, and enzymatic activity. To distinguish between local and global effects we compared fluorescence and near-UV CD data, which are specifically Trp-related, with data obtained from DSC and from far-UV CD measurements, which are not directly associated with Trp residues. In the kinetic experiments, local and global effects are distinguished by comparing the respective apparent free energies of the kinetic transition state that were obtained on the basis of stopped-flow fluorescence data.

It is worth mentioning that the present study, to our knowledge for the first time, deals with recombinant LA expressed in *Pichia pastoris*. The expression of LA in yeast has important advantages over the use of *Escherichia coli*, which was up to now the preferential host for the production of recombinant LA.[15,24–26] *P. pastoris* secretes natively folded GLA, and the extra N-terminal methionine is absent. This is important, as it has been shown that methionyl-LA has more solvent-accessible Trp residues, lower stability, and decreased calcium affinity compared to the authentic protein.[24,26] As will be shown further, the wild-type GLA expressed in *P. pastoris* has properties identical to those of authentic GLA from milk whey.

MATERIALS AND METHODS

Materials

Authentic goat α-lactalbumin (GLA) was prepared from fresh milk whey.[27] Restriction endonucleases, Klenow polymerase, T4 DNA ligase, and calf intestinal alkaline phosphatase were purchased from Boehringer-Mannheim or Promega. Primers were synthetized by Invitrogen. MES was obtained from Sigma. Bovine galactosyltransferase and UDP-galactose were from Sigma and ^{3}H-labeled UDP-galactose from Amersham.

Strains and Media

E. coli DH5α [*supE44 ΔlacU169(ϕ80laczΔM15) hsdR17 endA1 recA1 gyrA96 thi-1 relA1*] used as host strain for bacterial transformations and routine plasmid preparations was grown in Luria broth.[28]

For the expression of GLA mutants in *P. pastoris* the GS115 (*his4,* Mut$^+$) strain of the Pichia Expression Kit (Invitrogen®) was cultivated on RDB plates and YPD media as described by the manufacturer. For large-scale expression YPMG and YPMM (1% yeast extract, 2% peptone, 0.1 M MES, 0.1% threonine, 0.003% myoinositol, 0.003% pantothenate, 0.0225% leucine, 0.0045% adenine and uridine, 0.00227% amino acids: L-Trp, His, Arg, Met, Tyr, Lys, Phe, and 5% glycerol or 0.5% methanol, respectively) were used. The pH was adjusted at pH 7.

Construction of Wild-Type and Mutant GLA Genes

The pTZsA1T(ZSS)-plasmid containing the wild-type bovine α-lactalbumin gene (BLA gene) was constructed from the pTZs31T-plasmid[29] to allow the transfer of the BLA gene and its mutants, together with the prepro-α-mating factor, to the yeast vector pPIC9K (Pichia Expres-

sion Kit, Invitrogen®). Construction of the GLA gene from BLA was carried out in four subsequent steps using the QuikChange™ Site-Directed Mutagenesis Kit (Stratagene®, La Jolla, CA) as described by the manufacturer. The resulting plasmid, called pTZsA1TGLA(ZSS), was used as a template to construct two plasmids containing either the W60F or the W118F mutation. The double mutant W60/118F was constructed by ligation of the appropriate fragments resulting from the cleavage with *AvaI* and *XbaI* of the two plasmids containing the W60F or the W118F mutation. The correct construction of all the plasmids was verified by restriction digestion and sequence analysis. Plasmid DNA, used for DNA sequence analysis and for transformation, was prepared with the QIAGEN Plasmid Purification Kit (Qiagen, Westburg, Hilden, Germany). DNA sequence analysis was performed by Genome Express (Labo Grenoble, Meylan, France).

The shuttle vector pPIC9K was opened up by a double digestion with *BamHI* and *EcoRI*, with the loss of the α-mating factor preprosequence as a consequence. It was ligated to the *BamHI–EcoRI* fragment of pTZsA1TGLA-(ZSS) vector, which consisted of the α-mating factor preprosequence and the wild-type or the mutant GLA gene. The DNA sequence was analyzed to confirm the correct sequence of the inserts.

Transformation, Expression, and Purification

The recombinant plasmids were linearized with either *BglII*, *SacI*, or *SalI*. The linearized plasmids were used to transform *P. pastoris* cells according to the sferoplast method of Hinnen et al.[30] His^- RDB plates were used to screen for plasmid containing cells. After a qualitative prescreening, the best producing clones were grown in YPD at 28°C in shaker culture for 2 days.[31] The cells were resuspended in YPMG and incubated for 3 days at 28°C with shaking. Methanol induction started by changing the YPMG for YPMM-medium. To maintain induction the cells were supplied with methanol added to a final concentration of 1%. The culture was harvested after 5 days of growth and a RIA was used to estimate the expression yield of the recombinant protein.[28] The proteins were purified from the culture supernatant by means of hydrophobic interaction chromatography,[27] dialyzed and lyophilized. As *P. pastoris* secretes a certain percentage of glycosylated LA[32] the samples were further purified by affinity chromatography on a Con A Sepharose 4B column (Pharmacia). The nonglycosylated fraction was lyophilized.

Protein Characterization

The protein samples were run on a 10–20% tricine gradient gel (Invitrogen) in a Tris-tricine buffer. After fixation, the protein was detected with Coomassie PhastGel®Blue R (Pharmacia).

The proteins were subjected to electrospray ionization mass spectrometry (ESI-MS) on a Q-TOF mass spectrometer (Micromass, Manchester, UK) equipped with a nanoESI source, NanoMate100 (Advion Biosciences).

All experiments were performed in 10 mM Tris-HCl buffer, pH 7.5, containing 2 mM Ca^{2+}. The GLA concentration was determined by spectrophotometry using ε_{280} = 28,840 $(mol/L)^{-1}$ cm^{-1} for authentic and wild-type GLA, ε_{280} = 23,150 $(mol/L)^{-1}$ cm^{-1} for the W60F and W118F mutants and ε_{280} = 17,460 $(mol/L)^{-1}$ cm^{-1} for the double mutant W60/118F of GLA. The values of the molar extinction coefficients were calculated from the number of Trp, Tyr, and Cys residues.[33]

Spectroscopic Equilibrium Measurements

Circular dichroism measurements were made on a Jasco J-810 spectropolarimeter (Jasco, Tokyo, Japan), using an optical cell with path length of 0.02 cm for measurements in the far-UV region and 0.2 cm for measurements in the near-UV region. The GLA concentration used was approximately 30 μM.

Steady-state fluorescence was measured with a Perkin-Elmer LS55 Luminescence Spectrometer. The GLA concentration used was approximately 5 μM. Amounts of 3 mL of the degassed protein solutions were transferred into a 10 × 10 mm cell for fluorescence spectroscopy. The excitation wavelength was 280 nm, the bandpass for the excitation and emission slits was 5 and 3 nm, respectively. The fluorimeter was equipped with a magnetic stirrer mounted under the cell holder. The cell holder was thermostatted by circulating water from an external water bath. By means of a PID-control algorithm (Labview™) we imposed a stepwise heating program to the circulator thermostat: every 8th minute the temperature was increased by 3°C. Adjustment of the imposed temperature was controlled by a Pt100 sensor dipped in the solution. The registration of each fluorescence spectrum started 6 min after a new temperature was applied, 3 min after temperature equilibration of the sample is reached. The temperature did not vary more than 0.2°C during the registration of the spectrum. The temperature halfway this scan is noted.

The fractional change of the emission wavelength ($f_{fl,\lambda}$), used to plot apparent thermal transition curves, was defined as:

$$f_{fl,\lambda} = (\lambda_{obs} - \lambda_N)/(\lambda_U - \lambda_N)$$

where λ_{obs} is the observed wavelength of the emission maximum. At each temperature within the transition range the wavelengths of the emission maximum of native and unfolded LA, λ_N and λ_U, are extrapolated from the baselines before and after the thermal transition.

The fractional change of the fluorescence intensity ($f_{fl,int}$) was obtained by replacing the wavelengths by the corresponding intensities in the above equation.

Differential Scanning Calorimetry

Calorimetric scans were carried out on a MicroCal VP-DSC differential scanning calorimeter, using the software supplied by the manufacturer for data collection and analysis. The reference and the sample solutions were degassed for 15 min at room temperature prior to scanning at rates of 60°C/h. The protein concentration in the sample solutions was about 30 μM. The heat capacity of the sample protein was obtained by subtraction of a reference scan from the scan of the sample solution. Each heat

capacity scan was normalized by dividing the heat capacity scan of the sample by the number of moles of protein in the sample. The excess heat capacity function related to the protein unfolding was determined after subtraction of the baseline that takes into account the sigmoidal progression of the unfolding process.

Stopped-Flow Fluorescence Experiments

Folding and unfolding experiments were performed on an SX.18MV sequential mixing stopped-flow fluorescence spectrometer from Applied Photophysics (Leatherhead, UK). The stopped-flow unit and the observation cell with a 2-mm path length were thermostated by circulating water from a temperature-controlled bath. A monochromator was used for excitation at 280 nm and the fluorescence emission was measured using a high-pass filter with a 320-nm cutoff. The dead-time of the instrument was estimated to be about 2 ms. Typically, kinetics were measured 10–12 times, averaged, and analyzed as a sum of exponential functions by using the manufacturer's software. Chevron plots were constructed by plotting the logarithm of the rate constant as a function of denaturant concentration. All measurements were done at 25°C and pH 7.5 in 10 mM Tris and 2 mM Ca^{2+}. In the refolding experiments a solution of 0.5 mg/mL unfolded protein in 6 M GdnHCl was diluted 11-fold with refolding buffer containing various concentrations of GdnHCl. In unfolding experiments native protein (0.5 mg/mL) in buffer was diluted 11-fold with GdnHCl solutions of varying concentrations to give a final concentration between 2.8 and 6 M GdnHCl.

Kinetic Data Analysis

The transition curve expressed by the fraction of unfolded LA, f_{unf}, as a function of the concentration of denaturant, c, was obtained from the final fluorescence signal of the individual stopped-flow traces for refolding and unfolding experiments. The fractions for different mutants were fitted to the equation:

$$f_{unf} = \frac{\exp(-(\Delta G_{unf}^{H_2O} - m_{unf}\, c))}{1 + \exp(-(\Delta G_{unf}^{H_2O} - m_{unf}\, c))}$$

The fitting provides the numeric values of the unfolding free energy in the absence of denaturant, $\Delta G_{unf}^{H_2O}$, and of the cooperativity index for the transition, m_{unf}.[34] The unfolding free energy in presence of denaturant,ΔG_{unf}, is linearly dependent on GdnHCl concentration, c:

$$\Delta G_{unf} = \Delta G_{unf}^{H_2O} - m_{unf}\, c$$

The difference in the Gibbs free energy between the wild type and a particular mutant at a given GdnHCl concentration is defined as:

$$\Delta\Delta G_{unf} = \Delta G_{unf}^{wt} - \Delta G_{unf}^{mut}$$

The $\phi^{\ddagger}$-value of the transition state was calculated using the unfolding rates as follows:

$$\phi^{\ddagger} = 1 - \frac{\Delta\Delta G_{unf}^{\ddagger}}{\Delta\Delta G_{unf}} = 1 - \frac{RT\ln\left(\frac{k_{unf}^{mut}}{k_{unf}^{wt}}\right)}{\Delta\Delta G_{unf}}$$

where k_{unf}^{mut} and k_{unf}^{wt} are the unfolding rates of the mutant and the wild-type protein, respectively, at a given GdnHCl concentration. The $\phi^{\ddagger}$-values are summarized in Table V.

Lactose Synthase Assays

The lactose synthesis regulatory activities of the recombinant LAs were compared with the activity of authentic GLA using bovine β-galactosyltransferase (GTase) and UDP-galactose according to Brew et al.[35] The assays were performed in 200 μL of 50 mM Tris-HCl buffer (pH 7.5), 20 mM $MnCl_2$, 40 mM glucose, 0.3 mM UDP-galactose, 0.4 μCi UDP-[6-^{3}H]-galactose, 6 mU GTase, and 4–40 μg of recombinant protein. The amount of synthesized lactose was measured with the aid of a liquid scintillation counter (Packard Tri-Carb® 1900TR).

RESULTS

Characterization of GLA Mutants

Wild-type GLA and the three Trp mutants were expressed in transformed *P. pastoris*.

The level of expression of the recombinant proteins in the culture supernatant was measured by a RIA and amounts to about 40 mg · L^{-1} for both wild-type GLA and mutant W118F. The yield of W60F and W60/118F was in the range of 7 mg · L^{-1}. The recombinant proteins were purified from their respective supernatants by hydrophobic interaction chromatography. About 20% of wild-type GLA as well as of W118F obtained after this step was glycosylated. The mutants W60F and W60/118F were glycosylated for up to 40%. The nonglycosylated proteins were isolated by chromatography on a concanavalin A column. The purity of the final products was assayed by SDS-PAGE under reducing and nonreducing conditions. Under nonreducing conditions a small band at about 30kDa revealed the existence of a small fraction of dimeric GLA (~5%).

The recombinant proteins were further characterized by mass spectrometry. The mass spectrum of wild-type GLA exhibited a peak at 14,186 Da in correspondence with the mass of GLA purified from milk whey. The peaks for the mutants W60F and W118F were both at 14,148 Da. The double mutant W60/118F exhibited a peak at 14,109 Da. All masses agree with the respective theoretical amino acid composition and indicate that the obtained proteins are free of glycosylation and of any other expression-related modification.

Equal rates of synthesis of lactose are observed when authentic GLA, wild-type GLA, and the W60F mutant were used as activator of lactose synthesis. Only 4% of this rate is obtained when either W118F or W60/118F was assayed as activator. The latter result confirms previous observations indicating that the substitution of Trp118 always leads to a major reduction of the lactose synthase activity.[15]

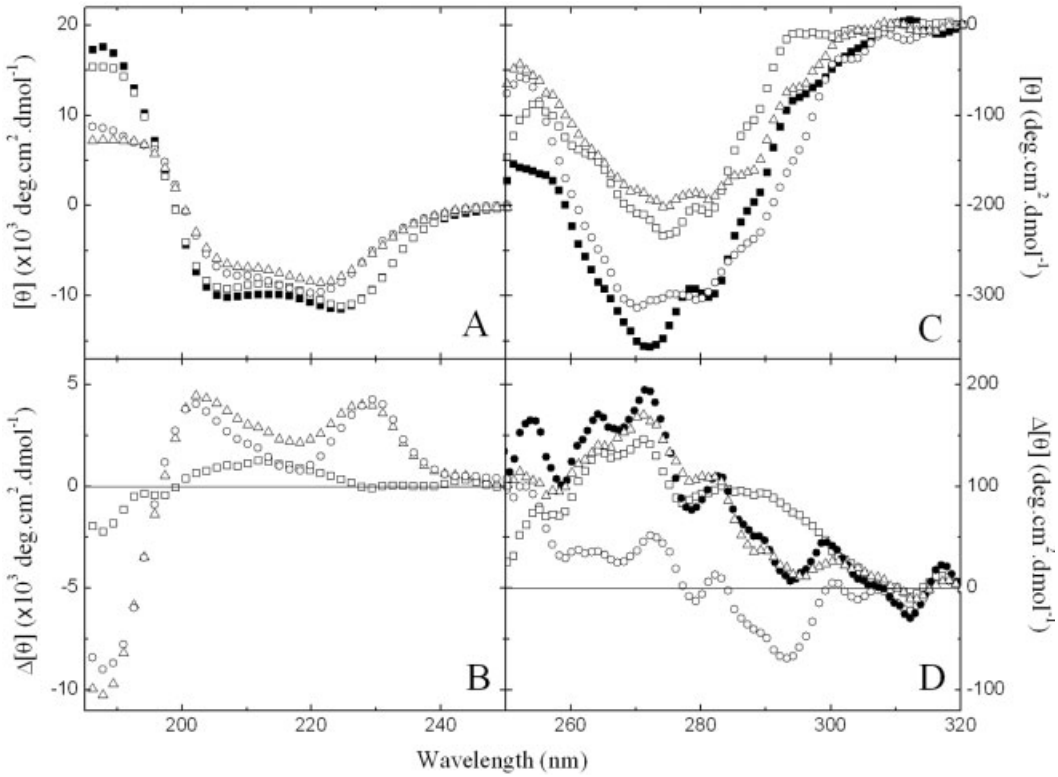

Fig. 2. (**A**) Far- and (**C**) near-UV CD spectra of wild-type GLA (■) and of the mutants W118F (□), W60F (○), and W60/118F (△) measured in 10 mM Tris-HCl, 2 mM $CaCl_2$, at pH 7.5 and 25°C. (**B**) Far- and (**D**) near-UV CD difference spectra between mutant W60F and wild-type (○), mutant W118F and wild-type (□), and between mutant W60/118F and wild type (△). In (**D**), the curve with symbol (●) corresponds to the sum of the near-UV CD difference spectra of which mutants W60F and W118F are involved.

CD Measurements

The secondary and tertiary structure of the authentic and the recombinant GLA was characterized by far- and near-UV CD spectroscopy in 10 mM Tris-HCl, 2 mM Ca^{2+} at pH 7.5 and 25°C. Under these conditions GLA is known to adopt the native conformation. The far-UV CD spectra of authentic and of wild-type GLA coincide with each other [Fig. 2(A), ■]. They show a broad band with two minima near 207 and near 224 nm, respectively, the first minimum having a lower intensity than the second one. The spectra also show a positive band near 190 nm. The observed spectral characteristics are typical for proteins with α/β character.[36] The substitution of Trp118 by Phe does not significantly alter the far-UV CD spectrum [Fig. 2(A), □]. In contrast, upon substitution of Trp60 by Phe, the positive band near 190 nm decreases in intensity [Fig. 2(A), ○ and △]. Also, the bands with negative ellipticity are less intense and the λ_{min} values shifted from 206.4 nm and 224 nm [Fig. 2(A), ■ and □] to 208.6 nm and 221 nm, respectively [Fig. 2(A), ○ and △]. The CD difference spectra between the various mutants and wild-type GLA [Fig. 2(B)] confirm earlier observations that the contributions of Trp60 are more complex than those of Trp118.[23,37] The difference may, at least partly, result from coupled oscillator interactions between Trp60 and neighboring chromophores.[38] Indeed, crystal structure analysis of LA has revealed that Trp60 forms an aromatic cluster with Tyr103 and Trp104.[3,5] This aromatic cluster is part of the interaction interface between the two lobes of LA. As the interactions between the subdomains are of great importance for the formation of a fixed native structure,[39,40] the substitution of Trp60 by Phe might influence the secondary structure of GLA also. In the difference spectra [Fig. 2(B), ○ and △] the bands with opposite signs could also be interpreted as a decrease of the α- or 3_{10}-helix content in the W60F and W60/118F mutants relative to the wild-type LA. Assuming that the ellipticity changes result exclusively from secondary structure changes, one can estimate the fractions of the different types of secondary structure from the CD spectra using specific deconvolution programs.[38] The results of a secondary structure calculation using the CDNN-program[41] show that, in so far as coupled oscillator interactions between Trp60 and the vicinal aromatic rings would not affect the far-UV CD signal, the α-helix content would decrease by about 8%, while that of the β-sheet structure would increase by 8–10% upon substitution of Trp60 by Phe.

In the near-UV region, the ellipticity data are more specifically related with aromatic contributions than in the far-UV. The negative ellipticity band near 270 nm is most pronounced for wild-type GLA [Fig. 2(C), ■]. This indicates that, at this wavelength, each Trp residue contributes to

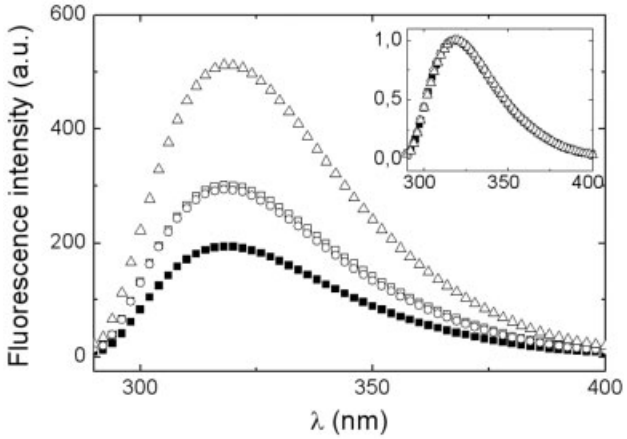

Fig. 3. Relative fluorescence intensity of wild-type GLA (■) and of the mutants W118F (□), W60F (○), and W60/118F (△) measured in 10 mM Tris-HCl, 2 mM $CaCl_2$, at pH 7.5 and 25°C. The excitation is at 280 nm and for each protein A_{280} equals 0.15, due to Trp absorption only, as explained in the text. The inset shows the normalized fluorescence spectra of the different proteins.

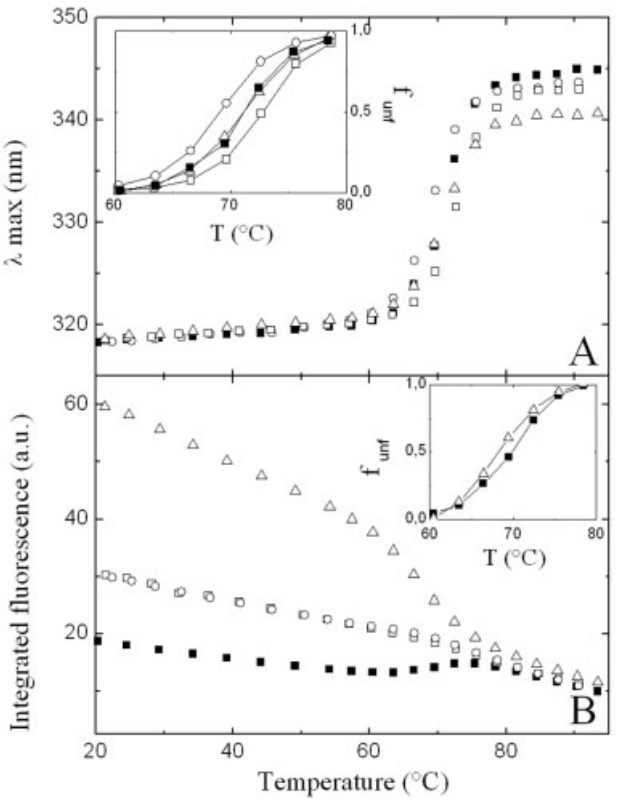

Fig. 4. (**A**) λ_{max} and (**B**) integrated fluorescence intensity as a function of temperature for wild-type GLA (■) and for the mutants W118F (□), W60F (○), and W60/118F (△) measured under the solvent conditions mentioned earlier. The inset of (**A**) shows in detail the fractional shift of the fluorescence ($f_{fl,\ \lambda}$) deduced from the change of λ_{max}. The inset of (**B**) shows in detail the fraction of apparently unfolded GLA ($f_{fl,int}$) derived from the change of fluorescence intensity.

the near-UV CD signal by a negative ellipticity value. Similar observations were made by Chakraborty et al.[23] on substitution of Trp by Phe in human LA. In contrast, in the range of 285–295 nm the ellipticity for wild-type GLA is less negative than for W60F [Fig. 2(C), ○] indicating that Trp60 contributes by a positive ellipticity band within this wavelength region. To clearly illustrate the specific contribution caused by the substitution of Trp60, we calculated the difference spectrum between W60F and wild-type GLA [Fig. 2(D), ○]. Figure 2(D) also shows the difference spectrum between mutant W118F and wild-type GLA [Fig. 2(D), □]. The substitution of Trp118 clearly results in two peaks of positive ellipticity: a first maximum is found near 270 nm, the second is near 290 nm. The positive difference peaks refer to negative contributions of Trp118. The calculated sum of both previous difference spectra [presented by ● in Fig. 2(D)] is in good accordance with the directly measured difference spectrum obtained by subtracting the spectrum of wild type from that of W60/118F GLA [Fig. 2(D), △]. This fair accordance suggests that the differences in the near-UV CD spectra of the various LA mutants are related to localized interactions of the aromatic residues rather than to long-range conformational changes. The simultaneous introduction of two mutations does not result in enhanced structural changes within the mutants: they behave as additive, which points to strictly localized effects in a globally conserved matrix.

Fluorescence Data

The fluorescence emission spectra of authentic and recombinant GLAs measured under conditions where they adopt the native state are presented in Figure 3. The excitation wavelength was 280 nm. To compensate for inner filter effects, the absorbance at 280 nm of the different solutions was adjusted at 0.150. Besides the Trp residues, also Phe, Tyr, and Cys absorb some light at 280 nm.[33] However, the shape of the different fluorescence spectra corresponds to that of Trp residues in an apolar medium. Also, upon unfolding of LA the emission maximum of the different spectra shifts to about 350 nm [Fig. 4(A)] as is expected for Trp residues that enter in aqueous medium. Therefore, the observed spectra of the different mutants can be attributed mainly to their Trp residues. For each LA mutant we calculated which fraction of light is absorbed by the Trp residues using extinction coefficients reported in ref. 33, and we adjusted the spectra in Figure 3 so as to represent intensities measured for equal Trp concentrations (2.1×10^{-5} mol/L). The integrated fluorescence intensities per unit of Trp are collected in Table I. These values times the number of Trp residues in the considered mutant represent the fluorescence per LA molecule (Table I, column 4). Mutant W60/118F with two residual Trp residues (Trp26 and -104), fluoresces more strongly than each of the mutants W60F and W118F that possess three residual Trps. In turn, the three Trps of W60F and W118F fluoresce more strongly than the four Trps of wild-type GLA. In a fluorescence study on mutants of human LA containing a single residual Trp, Chakraborty et al.[23] observed that, under native conditions, the fluorescence yield of the mutants with Trp60 and Trp118 is small compared to the fluorescence yield of mutants with Trp104. This was explained as due to the presence of strong

TABLE I. Integrated Fluorescence Intensity (Arbitrary Units) of Wild-Type GLA and of Its Mutants at Comparable Concentrations, at 25°C and pH 7.5, in 10 mM Tris-HCl Containing 2 mM $CaCl_2$

Mutant	Residual Trp residues	Integrated fluorescence/ Trp	Integrated fluorescence/ GLA
Wild type	26, 60, 104, 118	18.0	72.0
W60F	26, 104, 118	29.2	87.6
W118F	26, 60, 104	30.2	90.6
W60/118F	26, 104	58.2	116.4

GLA, goat α-lactalbumin.

quenchers nearby the former Trp residues. They also observed that the fluorescence yield of wild-type human LA is smaller than that of the mutant containing the single Trp104. This phenomenon was considered to be mediated by energy transfer between Trp104 and a Trp residue that undergoes further quenching. Trp60 was designated as the mediator for this indirect quenching in accordance with an earlier report.[42] Our data (Table I, column 4) indicate that both Trp118 and Trp60 are about equally effective in the quenching of the fluorescence of both Trp26 and -104.

Starting from W60/118F, the integrated fluorescence intensity per protein molecule is reduced by 26 to 29 arbitrary units by the addition of the first supplemental Trp (in W60F or W118F) and only by 15 to 18 arbitrary units by the addition of the second supplemental Trp (wild-type GLA). This decrease of increment of the quenching effect supports the idea that in native LA, Trp26–104 behaves as a resonance couple and not as two individually emitting units. Indeed, if Trp26 and Trp104 would behave as two separate emission units, the quenching effect mediated by the introduction of the vicinal Trps (Trp60 is vicinal to Trp104 and Trp118 is vicinal to Trp26) would not be influenced by their sequence of addition.

It is worthy of notice that, although the emission intensities of the native GLA mutants are very different, the shape of the different spectra is very similar (Fig. 3). To better visualize the latter property the different spectra are rescaled to the same maximum (inset of Fig. 3). The excellent similarity is readily explained by the fact that each spectrum reflects fluorescence of the same Trp residues. As mentioned previously, Trp60 and -118 do not importantly contribute to the fluorescence of native W118F, nor of native W60F or wild-type GLA. Therefore, in each of these molecules the fluorescence mainly results from Trp26 and/or -104. The fluorescence of those buried Trp residues is at the short wavelength side of the emission spectrum and exhibits a maximum near 320 nm.

Figure 4(A) shows the change of wavelength of the emission maximum for GLA and its mutants as a function of temperature. For the reasons mentioned above, the emission maximum of all GLA mutants is near 320 nm at temperatures below the transition temperature, $T_{m,\mathrm{Fl}}$. At temperatures above $T_{m,\mathrm{Fl}}$ the emission maximum of the different mutants and of wild-type GLA shifts to longer wavelengths (340–345 nm) and finally differ mutually by several nm [Fig. 4(A)]. It is worth notice that in the thermally unfolded state, especially the double mutant W60/118F has a lower λ_{max} (340 nm) than authentic and wild-type GLA (345 nm). This suggests that, in the unfolded form, the Trp26 and Trp104 residues remain somewhat more protected from solvent than Trp60 and/or Trp118, which are additionally present in the other constructs. Indeed Trp26 and -104 belong to the α-helical domain of GLA. Moreover, Trp26 belongs to one of the major α-helices (helices 23–34). α-Helices are known to resist strongly denaturing conditions.

The fractional change of the wavelength maximum upon transition is easily determined with good accuracy for the various recombinant LA mutants. The resultant curves [Fig. 4(A), inset] show symmetry. The midpoints represent the apparent transition temperatures ($T_{m\ \mathrm{Fl},\lambda}$) and are listed in Table II.

Below the transition temperature, the integrated fluorescence intensity of all types of recombinant GLA studied decreases upon heating [Fig. 4(B)]. The decrease corresponds with the expected thermal quenching. Within the domain of the thermal transition the fluorescence of wild-type GLA shows a sigmoid increase, while the transition curve of theW60/118F mutant is characterized by an enhanced, sigmoid decrease. The effect of thermal transition on the fluorescence intensity of authentic and of wild-type GLA is dominated by a strong reduction of the close contact between Trp60 and -118, respectively, and their putative quenchers. Also, the indirect quenching of Trp26 and -104, which is mediated by the former Trps, decreases when the compact protein looses its native tertiary structure. In contrast, due to the absence of quenching effects in native W60/118F, the effect of the thermal transition on the fluorescence intensity of this mutant is dominated by the loss of apolar environment of Trp26 and -104 and, therefore, by an increase of contact quenching by the polar medium. The fractional changes within the transition region are presented in the inset of Figure 4(B). The midpoints ($T_{m\ \mathrm{Fl,int}}$) are listed in Table II.

DSC

The molar heat capacity of GLA and its mutants as a function of temperature is shown in Figure 5. After subtraction of the respective baselines, which take into account the progression of the denaturation process, the profiles of the excess heat capacity as a function of temperature result in symmetric Gauss curves with maxima at the respective transition midpoint temperatures, $T_{m,\mathrm{DSC}}$ (Table II). Due to their perfect symmetry the curves fit the van't Hoff equation for a two-state transition. The related molar enthalpy (ΔH_{unf}) and entropy changes (ΔS_{unf}) are derived from the curves using software for data analysis provided by the manufacturer. The respective ΔH_{unf} and ΔS_{unf} values are collected in Table III. Under the conditions of our experiments (Tris-HCl buffer of pH 7.5 at 25°C in the presence of 2 mM Ca^{2+}) the $T_{m,\mathrm{DSC}}$ and ΔH_{unf} values of authentic and wild-type GLA are 71.1 ± 0.1°C and 351 ±1 $kJ.mol^{-1}$, respectively. These values are clearly higher than the corresponding ones of bovine LA

TABLE II. Unfolding Temperature (°C) Deduced from the Transition Midpoint of Thermal Unfolding of GLA and Its Trp Mutants

	$T_{m,\mathrm{Fl}\,\lambda}$	$T_{m,\mathrm{Fl\,int}}$	$T_{m,\mathrm{DSC}}$	$T_{m,\mathrm{Fl}\,\lambda}$–$T_{m,\mathrm{DSC}}$
Authentic	70.7 ± 0.4		71.0 ± 0.2	−0.3
Wild type	71.2 ± 0.2	69.9[a]	71.1 ± 0.2	+0.1
W118F	73.0 ± 0.2	/	71.5 ± 0.2	+1.5
W60F	69.2 ± 0.2	/	67.9 ± 0.2	+1.3
W60/118F	71.0 ± 0.3	68.0 ± 0.3	68.1 ± 0.2	+2.9

The unfolding temperature is deduced from shifts of the fluorescence wavelength ($T_{m,\mathrm{Fl}\,\lambda}$), the fluorescence intensity ($T_{m,\mathrm{Fl\,int}}$) and from heat capacity changes ($T_{m,\mathrm{DSC}}$), respectively.
[a]The transition curve from which this value is deduced did not fit to the van't Hoff equation.

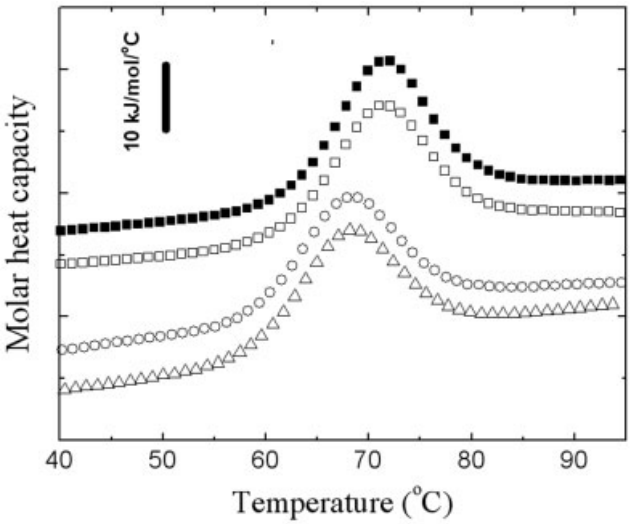

Fig. 5. Molar heat capacity as a function of temperature for wild-type GLA (■) and for the mutants W118F (□), W60F (○), and W60/118F (△) measured under the solvent conditions mentioned earlier.

TABLE III. Thermodynamic Parameters for Thermal Unfolding of Authentic and of Recombinant GLA in the Presence of 2 mM Ca^{2+} and 10 mM Tris-HCl at pH 7.5 at 25°C

	$T_{m,\mathrm{DSC}}$ (°C)	ΔH_{unf} ($\mathrm{kJ \cdot mol^{-1}}$)	ΔS_{unf} ($\mathrm{kJ \cdot mol^{-1} \cdot K^{-1}}$)
Authentic	71.0 ± 0.2	351.5 ± 1.7	1.021 ± 0.006
Wild type	71.1 ± 0.2	349.4 ± 0.9	1.015 ± 0.003
W118F	71.5 ± 0.2	344.4 ± 0.8	0.999 ± 0.003
W60F	67.9 ± 0.2	320.2 ± 0.6	0.939 ± 0.002
W60/118F	68.1 ± 0.2	324.0 ± 1.0	0.949 ± 0.004

The parameters are obtained by fitting the curves of the excess heat capacity (DSC) to the van't Hoff equation for a two-state transition.

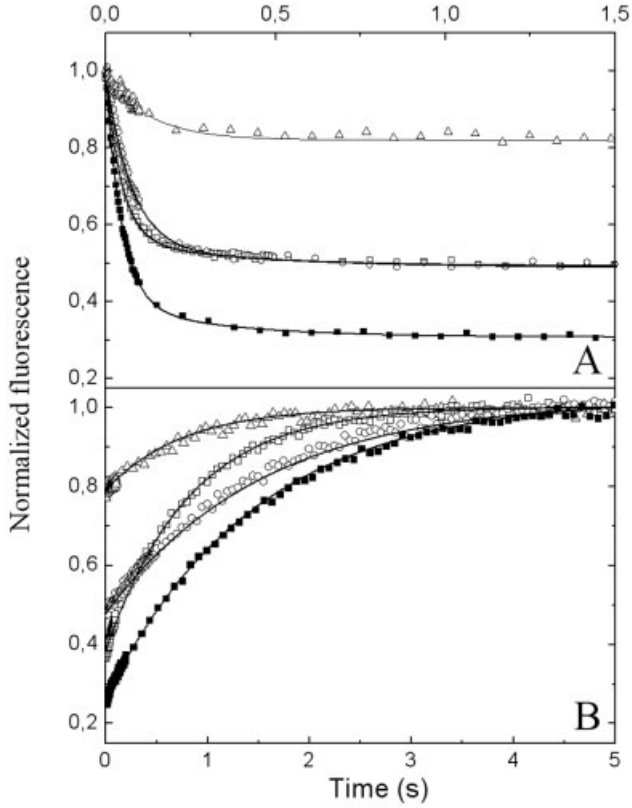

Fig. 6. Time course of (**A**) kinetic refolding after dilution from 6 to 0.54 M GdnHCl and of (**B**) kinetic unfolding after addition of GdnHCl to a final concentration of 5.05 M for wild-type GLA (■) and for the mutants W118F (□), W60F (○), and W60/118F (△) monitored by stopped-flow fluorescence. The other environmental conditions are: pH 7.5, 25°C and 2 mM $CaCl_2$. The continuous line represents a double (**A**) and a single (**B**) exponential fit through the experimental data. For each mutant the fluorescence values are relative to those of the unfolded state, the fluorescence of which has been set to unity.

(BLA). Under identical conditions $T_{m,\mathrm{DSC}}$ and ΔH_{unf} of BLA is 68.7°C and 318 $\mathrm{kJ \cdot mol^{-1}}$, respectively.[43–45] In previous work we already observed that at 25°C the ΔH values for the unfolding of Ca^{2+}-bound GLA are larger than those of BLA: 216 $\mathrm{kJ \cdot mol^{-1}}$ and 196 $\mathrm{kJ \cdot mol^{-1}}$, respectively.[46] Visibly, the higher enthalpy of unfolding of GLA compared to that of BLA is a stabilizing factor over the whole temperature range.

The substitution of Trp60 by Phe reduces ΔH_{unf} by about 20–30 $\mathrm{kJ \cdot mol^{-1}}$ and shifts $T_{m,\mathrm{DSC}}$ of GLA from 71.1 to 67.9°C; the influence of the Trp118 substitution on $T_{m,\mathrm{DSC}}$ and on ΔH_{unf} is clearly smaller.

Refolding and Unfolding Kinetics

Figure 6(A) shows the kinetic traces obtained in a refolding buffer without additional denaturant leading to a final concentration of 0.54 M GdnHCl. For each of the proteins, a substantial fluorescence intensity change (33–41%) occurs during the dead-time of the instrument (2 ms). The observable part of the signal evolves according to a

TABLE IV. Refolding and Unfolding Parameters of GLA and Its Trp Mutants at pH 7.5, 2 mM $CaCl_2$ and 25°C

Mutant	A_1 (%)	k_1 (s^{-1})	A_2 (%)	k_2 (s^{-1})	k_{unf} (s^{-1})
Authentic	88.5	19.5	11.5	2.21	0.54
Wild type	90.4	20.8	9.6	2.06	0.68
W118F	89.3	21.7	10.7	2.86	1.23
W60F	86.7	11.9	13.3	2.01	0.65
W60/118F	80.5	12.8	19.5	2.05	1.33

The refolding parameters are obtained in 0.54 M GdnHCl. A_1 and A_2 represent the fractional amplitudes of the signal observed after dead time, k_1 and k_2 are the respective refolding rate constants. The unfolding rate constant k_{unf} is obtained in 5.05 M GdnHCl. The unfolding fits a mono-exponential decay. No burst-phase intermediate has been observed upon unfolding.

bi-exponential function with rate constants k_1 and k_2 (Table IV). In absolute terms the fluorescence intensity change during refolding is largest in the wild-type sample, the fluorescence of which is largely quenched in the native state as has been concluded previously from the static fluorescence spectra (Fig. 4). As can be derived from the different final intensity levels of the native protein [Fig. 6(A)], the fluorescence intensity change during refolding is smaller in both single mutants and is the smallest in the double mutant.

For the wild-type protein, the bi-exponential fit gives refolding rates of $k_1 = 20.8 \pm 0.5\ s^{-1}$ and $k_2 = 2.06 \pm 0.1\ s^{-1}$ with fractional amplitudes of 90.4 and 9.6% of the observed signal changes. The mutation of Trp118 leaves these parameters practically unchanged. Mutation of Trp 60, however, reduces k_1 to $11.9 \pm 0.5\ s^{-1}$ without significant change of k_2 and of the contributions of the respective amplitudes. The double mutant W60/118F conserves the k_1 value ($12.8 \pm 0.5\ s^{-1}$) of W60F but shows a modified distribution of the amplitudes. It must be said, however, that in this case, the calculated fractions refer to a much smaller total amplitude and, therefore, are less precise.

In Figure 6(B), the normalized fluorescence intensity is depicted for the unfolding process to a final concentration of 5.05 M GdnHCl. In general, when a protein unfolds, Trp residues become increasingly water accessible and the intensity of the fluorescence emission of the unfolded protein decreases due to a higher rate of internal conversion.[47] This is not the case in GLA and its Trp mutants; the intensity observed in the unfolded state increases with respect to the intensity in the native state. This effect can be interpreted as resulting from the loss of internal quenching by surrounding His residues (His32, His68, and His107) and disulfide bridges (Cys6–Cys120, Cys28–Cys111, Cys61–Cys77, and Cys73–Cys91) upon unfolding of the protein.[48] Interestingly, when Trp118 and Trp60 are mutated, the difference in fluorescence level between the native and unfolded state decreases. This means that the remaining Trp residues (Trp26 and Trp104) are probably quenched by the neighboring His residues (His32 and His107), as it has been reported that both residues are somewhat shielded from solvent at high pH (6.5–8).[14,49]

For all samples, the evolution towards the unfolded state, which is set to show the same final fluorescence intensity, can be described by a single exponential function (Table IV). Mutation of Trp 118 causes a nearly doubling of the speed of the unfolding process that is also observed in the double mutant, while the replacement of Trp 60 has practically no effect.

Chevron Plots

The kinetics of folding and unfolding of authentic GLA has recently been studied extensively.[50] In this work, the refolding and unfolding kinetics of wild-type GLA and the different mutants were measured at various concentrations of GdnHCl. In all cases, the major rate constant k_1 shows a V-shaped dependence on GdnHCl concentration (Fig. 7). The minimum of this chevron plot corresponds with the midpoint of transition upon chemical denaturation as it can be derived from equilibrium measurements. In this way, the c_m was determined to be 3.6 M GdnHCl for wild-type GLA. The replacement of Trp118 does not significantly affect this value (Fig. 7), indicating that the stability towards chemical denaturation of the protein has not been changed by this mutation. This observation is in accordance with our previous results on the thermal stability obtained by DSC (Fig. 5). In W60F and in the double mutant (Table V), on the other hand, the minimum shifts to 3.1 M, referring to a lower stability of these proteins. These observations correspond with the DSC results, where for both these mutants $T_{m,DSC}$ also shifts to a lower value.

The thermodynamic parameters can be calculated from the N → U transition curves resulting from the kinetic measurements that were depicted in Figure 8. These values are brought together in Table V. The continuous lines in Figure 8 are the curves theoretically drawn with the parameters obtained from the fit. In all cases the m_{unf}-values determined from the kinetic data are very similar, indicating that the degree of solvent exposure of the native and denaturated states has not been significantly altered by the respective mutations.

DISCUSSION

In GLA we substituted Trp60 and -118, respectively, for Phe. Both Trps are located in flexible but different regions of the protein. As Trp residues are extremely sensitive reporters in near-UV CD and fluorescence spectroscopy, we expected that comparison of the characteristics derived from these spectra under equilibrium and kinetic conditions would supply information on local organization and stability within the LA molecule. To judge whether the changes induced by thermal or chemical denaturation are local or global, we also used techniques that are not directly Trp-related such as far-UV CD and DSC.

The substitution of Trp118 by Phe, which occurs in a flexible region of the α-helical domain, strongly inhibits the ability of LA to act as a lactose synthase modulator. This result perfectly agrees with observations of Grobler et al.,[15] who found that mutation of residue 118 reduces the affinity for galactosyltransferase. The former substitution does not influence the far-UV CD spectrum [Fig. 2(A)], indicating that the secondary structure of LA is not

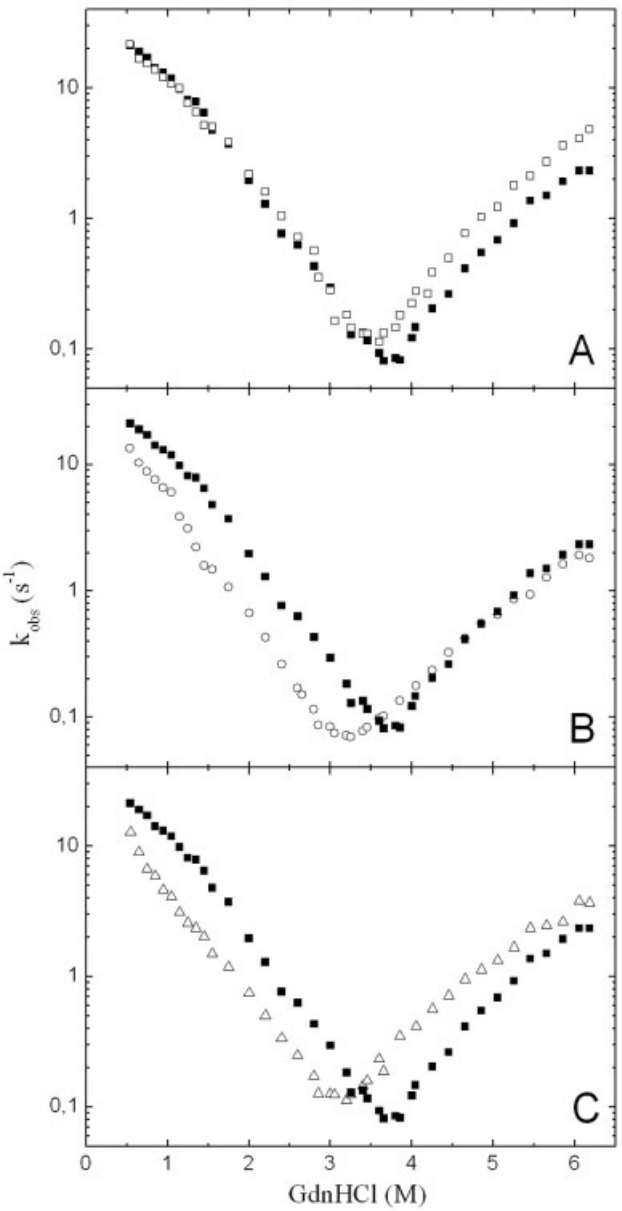

Fig. 7. Observed rate constants of refolding (left branch) and unfolding (right branch) for wild-type GLA (■) with respect to the mutant (**A**) W118F (□), (**B**) W60F (○), and (**C**) W60/118F (△) as a function of the denaturant concentration at pH 7.5, 25°C and 2 mM $CaCl_2$.

affected. Also, as can be derived from DSC, the thermodynamic characteristics (ΔH_{unf} and ΔS_{unf}) and the associated transition temperature ($T_{m,\mathrm{DSC}}$) of GLA are hardly affected by this mutation (Table III).

The β-domain of LA is known to represent another region of relatively poor stability and high flexibility.[8] The substitution within that region of Trp60 by Phe has no measurable effect on the lactose synthase activation by GLA, indicating that at least the region that interacts with galactosyl transferase conserves its native conformation. As mentioned above, the latter region is located at the surface of the α-helical domain. A second indication that the α-helical domains of W60F and of W60/118F mainly conserve their native structure comes from the shape of the fluorescence spectrum (inset of Fig. 3). The fact that neither the positions nor the shapes of these spectra differ, is a strong indication that the structure around Trp26 and -104 is conserved. These residues are located within the α-domain. Therefore, the differences between the far-UV CD spectrum of W60F and that of wild-type GLA [Fig. 2(A) and (B)] must be interpreted as mainly due to coupled oscillator interactions between Trp60 and the neighboring Tyr103 and Trp104.[23,37] The results from DSC scans indicate that substitution of Trp60 by Phe leads to a decrease of the global stability. Indeed, the transition temperature (Table III) has decreased from about 71.1°C for wild-type GLA to 67.9°C for W60F and to 68.1°C for W60/118F. The loss of stability is interpreted as due to the weakened interactions in the aromatic cluster rather than to changes in the secondary structure. From the thermodynamic point of view, this decrease of $T_{m,\mathrm{DSC}}$ is effectuated by a reduction of ΔH_{unf} and is not compensated by the associated reduction of ΔS_{unf} (Table III).

The question remains to what degree the differences between T_m values derived from fluorescence measurements and from DSC are indicative for local versus global conformational changes. In answer to that question, we compared the transition temperature deduced from DSC ($T_{m,\mathrm{DSC}}$) with that deduced from fluorescence wavelength shift ($T_{m,\mathrm{Fl}\,\lambda}$) and fluorescence intensity ($T_{m,\mathrm{Fl\,int}}$), respectively. As mentioned earlier, the thermal denaturation of each LA mutant results in a pronounced shift of its Trp emission maximum towards longer wavelengths [Fig. 4(A)]. Its evolution as a function of temperature can be easily derived. Each of the obtained transition curves [Fig. 4(A), inset] could be fitted to the van't Hoff equation and the deduced ΔH-values (not shown) correspond with those of DSC. Therefore, the midpoints of these transition curves, referred to as $T_{m,\mathrm{Fl}\,\lambda}$ in Table II, are frequently used as reliable transition temperatures.[51,52] The calculated temperature differences ($T_{m,\mathrm{Fl}\,\lambda} - T_{m,\mathrm{DSC}}$) amount to +0.1°C for wild-type GLA, +1.3°C for W60F, +1.5°C for W118F, and +2.9°C for the double mutant W60/118F (Table II). Seemingly, the differences could refer to a retarded exposure to solvent of the two remaining Trp residues, Trp26 and Trp104, at the core of the α-domain. However, the above conclusion assumes that additivity exists for the shift of the wavelength maximum, that is, that the observed wavelength maximum equals the sum of the wavelength maximum for the fractions of protein in the native and that for protein in the unfolded state. This consideration obliged us to search for the possible causes of nonadditive behavior and to examine other, more reliable reasons why ($T_{m,\mathrm{Fl}\,\lambda} - T_{m,\mathrm{DSC}}$) increases when Trp60 and Trp118 are mutated in GLA. The solution of the problem is given by the observation that the increase of the value ($T_{m,\mathrm{Fl}\,\lambda} - T_{m,\mathrm{DSC}}$) (Table II) also follows the increase of the difference between the fluorescence intensity of the native and that of the unfolded state [Fig. 4(B)]. As has been stated by Eftink,[47] the emission maximum of a mixture of overlapping fluorescence spectra will be weighted toward the dominantly emitting species. Therefore, by their larger

TABLE V. Thermodynamic Parameters for the GdnHCl-Induced Unfolding of Wild-Type GLA and Its Mutants at 25°C, pH 7.5, in 10 mM Tris-HCl Containing 2 mM $CaCl_2$

	c_m (mol · L^{-1})	$\Delta G_{unf}^{H_2O}$ (kJ · mol^{-1})	m_{unf} (kJ · mol^{-1} · M^{-1})	$\Delta G_{unf}^{5.05Gd\ nHCl}$ (kJ · mol^{-1})	$\Delta\Delta G_{unf}^{5.05GdnHCl}$ (kJ · mol^{-1})	$\phi^{\ddagger}$
Wild type	3.6 ± 0.1	44.2 ± 2.5	12.2 ± 1.2	−17.6	—	—
W118F	3.5 ± 0.1	44.0 ± 2.0	12.6 ± 1.4	−19.8	2.2	0.07
W60F	3.1 ± 0.1	41.2 ± 1.6	13.1 ± 1.2	−25.1	7.5	0.94
W60/118F	3.0 ± 0.1	40.4 ± 1.3	13.2 ± 1.1	−26.4	8.8	0.97[a]

c_m is the midpoint concentration of the GdnHCl-induced unfolding, $\Delta G_{unf}^{H_2O}$ and $\Delta G_{unf}^{5.05GdnHCl}$ are free energies for unfolding in the absence of denaturant and in 5.05 M GdnHCl, respectively. $\Delta\Delta G_{unf}^{5.05GdnHCl}$ is the difference between the unfolding free energy of wild-type and mutant GLA in 5.05 M GdnHCl. m_{unf} is the cooperativity index. The $\phi^{\ddagger}$-values are calculated as described in Materials and Methods.
[a]This value has been calculated in relation to k_{unf} and to ΔG_{unf} of mutant W118F and thus is illustrative for the influence of the mutation of Trp60.

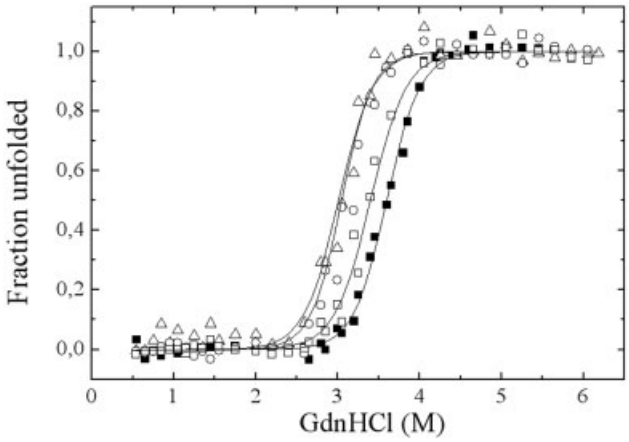

Fig. 8. Unfolded fraction of wild-type GLA (■) and of the mutants W118F (□), W60F (○), and W60/118F (△) as a function of the denaturant concentration at pH 7.5, 25°C and 2 mM $CaCl_2$. The data are calculated from the final values of the fluorescence intensity measured during folding and unfolding. The solid lines represent fits based on a two-state model.

fluorescence intensities in the native state than in the unfolded state, the mutants W60F and W118F have to unfold to a larger extent than wild-type GLA to realize a shift of the wavelength maximum. For the same reason mutant W60/118F has to unfold to a larger extent than these single mutants. Thus, the value ($T_{m,Fl\ \lambda} - T_{m,DSC}$) for a Trp mutant of GLA is, at least partially, related with the difference between the fluorescence intensity of the native and the unfolded state.

In contrast to the wavelength shift, the global fluorescence intensity is the sum of all fractional contributions. Therefore, the value ($T_{m,Fl\ int} - T_{m,DSC}$) may offer a better indication for the occurrence of local rearrangements upon thermal unfolding than ($T_{m,Fl\ \lambda} - T_{m,DSC}$). When looking at the change of the fluorescence intensity, only in the case of wild-type GLA and of W60/118F a clear transition is observed [Fig. 4(B)]. For both these LAs, $T_{m,Fl\ int}$-values (Table II) are obtained at the midpoints of the corresponding transition curves [Fig. 4(B), inset]. Actually, only the $T_{m,Fl\ int}$ of W60/118F could be determined with satisfactory confidence. Indeed, only for that mutant the transition curve could be fitted to the van't Hoff equation and the deduced ΔH-value corresponded with that of DSC. The resulting ($T_{m,Fl\ int} - T_{m,DSC}$)-value is nearly zero. As a consequence, no intermediate state with locally rearranged Trp residues can be detected upon thermal unfolding. However, it is worth to remember that, above 70°C, the unfolded LA keeps a nucleus containing of Trp26 and -104 that is partly protected from solvent as has been concluded from the incomplete fluorescence shift of W60/118F [Fig. 4(A)].

The refolding and unfolding kinetics of wild-type GLA and of the Trp mutants upon dilution with or addition of GdnHCl (Figs. 6 and 7) as well as the associated equilibria between the folded and the unfolded state (Fig. 8) have been followed by measuring the evolution of the fluorescence intensity as a function of time. At 25°C, 2 mM Ca^{2+} and 0.54 M GdnHCl, the respective rate constants for the biphasic refolding reactions of mutant W118F and of wild-type GLA are very similar (Table IV), while the unfolding reaction of the mutant in 5.05 M GdnHCl is nearly twice as fast (Table IV). This suggests that, at room temperature, the stability difference can be related to the increased unfolding rate of W118F. The difference in activation free energy between the wild-type and the mutant, $\Delta\Delta G_{unf}^{\ddagger}$, is known to be given by the ratio of the unfolding rate constants as:

$$\Delta\Delta G_{unf}^{\ddagger} = RT\ln\left(\frac{k_{unf}^{mut}}{k_{unf}^{wt}}\right)$$

where k_{unf}^{mut} and k_{unf}^{wt} represent the unfolding rate constants for the mutant and wild-type GLA, respectively. Because k_{unf}^{mut} is nearly two times larger than k_{unf}^{wt} at 5.05 M GdnHCl, $\Delta\Delta G_{unf}^{\ddagger}$ is estimated to be 1.8 kJ/mol, and this value is nearly identical with the $\Delta\Delta G_{unf}$ (2.2 kJ/mol) at the same concentration of denaturant (Table V). Equivalent results are obtained with other GdnHCl concentrations. The fact that identical values are obtained for $\Delta\Delta G_{unf}^{\ddagger}$ and for $\Delta\Delta G_{unf}$ on substituton of Trp118 by Phe ($\phi^{\ddagger} = 0.07$), means that in the transition state the structure around the mutation site is identical with that in the denatured state, that is, not organized.[53–55] This result also indicates that the initiation site for refolding of GLA is not located in the region near Trp118. It is in agreement with previous studies on bovine LA in which it has been shown that the structure around the 6–120 disulfide bond, which is vicinal to Trp118, is not yet organized in the transition state of refolding.[56]

In contrast with W118F, the $\Delta\Delta G_{unf}^{\ddagger}$ of the W60F variant is estimated to be 0 kJ/mol, because its unfolding rate

remains unchanged by the latter mutation [Table IV, Fig. 7(B)], whereas $\Delta\Delta G_{unf}$ amounts to 7.5 kJ/mol (Table V). The corresponding $\phi^{\ddagger}$-value equals 0.94. This means that the structure around the mutation site is similarly organized in the native state and in the transition state. The findings strongly indicates that the interface between the α- and β-domain is organized in the transition state.[57]

Recently Saeki et al.[37] studied a large number of GLA mutants, including W60A, all of them carrying an N-terminal methionine. They followed the GdnHCl-induced unfolding of the recombinant proteins with equilibrium and stopped-flow CD techniques. The similarity of the $\Delta\Delta G^{\ddagger}_{unf}$ and $\Delta\Delta G_{unf}$ values for their mutant W60A indicates that the mutation site is not involved in the formation of an intermediately folded state. Their results furthermore demonstrate that the native structure around the Ca^{2+}-binding site of mutant D87N is fully formed in the transition state and that the mutation sites of I55V, I89V, V90A, and I95V are partly organized. The latter mutations are located in the interface between the C-helix and the β-domain. Trp60 is similarly located in the β-domain and keeps contact with the C-helix.[3] According to Saeki et al.,[37] the mutation site of their protein, W60A, is not organized in the transition state, whereas in our mutant, W60F, the similar region has native-like structure. A possible reason for this striking difference in unfolding behavior of these two mutants could reside in the difference in steric properties and hydrophobic character of Phe and Ala. Indeed, Trp60 is part of the aromatic cluster II [3,15] and the propensity to form hydrophobic clusters has been designated as being important for the initial collapse upon protein folding and for the retention of an intermediately folded structure upon unfolding.[58] Obviously, in contrast to Phe, the hydrophobic character of Ala in W60A is not strong enough to take over the role of Trp during the unfolding process. The marked difference of $\Delta\Delta G^{\ddagger}_{unf}/\Delta\Delta G_{unf}$ between W60F and W60A indicates that the nature of the involved amino acids strongly determines the extent and the tightness of packing of the intermediately formed folding nuclei. This result demonstrates that the role of these amino acids is not limited to the final docking processes resulting in the native state, but also involves the earlier phases of folding.

CONCLUSION

In GLA, which contains four Trp, the mutation of Trp60 and/or Trp118 by Phe has allowed us to observe that these Trp residues are both quenched in native GLA. Moreover, both residues equally contribute to the quenching of Trp26 and Trp104, which behave as a resonance couple. In our search to discriminate between global and local rearrangements upon thermal denaturation we demonstrated that the differences between the mutants, which were obtained from measurements of the value $(T_{m,\mathrm{Fl}\ \lambda} - T_{m,\mathrm{DSC}})$, are related to differences in quenching and, therefore, to the different fluorescence intensities of the Trp residues. The fact that equal values were obtained for $T_{m,\mathrm{Fl\ int}}$ and $T_{m,\mathrm{DSC}}$ of the W60/118F mutant, allowed us to conclude that no local folding events occurred upon thermally induced unfolding of this Ca^{2+}-bound mutant. In addition, this mutant allowed us to observe that unfolded GLA, above 70°C, conserves a nucleus consisting of Trp26/104 that is partly protected from solvent.

In contrast, stopped-flow fluorescence measurements of chemically induced folding/unfolding reactions of these mutants have shown the direct behavior of the intermediate environments of Trp60 and -118. Short range rearrangements are indeed deduced by $\phi^{\ddagger}$-value analysis, that is, by comparing the apparent free energy changes needed to reach the kinetic transition and the unfolded state, respectively. Specifically, our findings indicate that in the kinetic transition state the mutation site of W118F looses its native conformation while the mutation site of W60F is conserved.

ACKNOWLEDGMENTS

We thank Wim Noppe, Linda Desender, Christiane Duportail, and Nicole Holvoet for their help with construction, expression, and purification of mutant α-lactalbumins. We are grateful to Bart Devreese and Kris De Vriendt of the laboratory for Protein Biochemistry and Protein Engineering of the University of Ghent, for molecular mass determinations.

REFERENCES

1. Hill RL, Brew K. Lactose synthetase. Adv Enzymol 1975;43:411–490.
2. Bell JE, Beyer TA, Hill RL. Kinetic mechanism of bovine milk galactosyltransferase—role of alpha-lactalbumin. J Biol Chem 1976;251:3003–3013.
3. Acharya KR, Stuart DI, Walker NPC, Lewis M, Phillips DC. Refined structure of baboon alpha-lactalbumin at 1.7-Å resolution—comparison with c-type lysozyme. J Mol Biol 1989;208:99–127.
4. Kronman MJ, Sinha SK, Brew K. Characteristics of the binding of Ca^{2+} and other divalent metal-ions to bovine alpha-lactalbumin. J Biol Chem 1981;256:8582–8587.
5. Chrysina ED, Brew K, Acharya KR. Crystal structures of apo- and holo-bovine alpha-lactalbumin at 2.2-Å resolution reveal an effect of calcium on inter-lobe interactions. J Biol Chem 2000;275:37021–37029.
6. Kronman MJ. Metal-ion binding and the molecular conformational properties of alpha-lactalbumin. Crit Rev Biochem Mol Biol 1989;24:565–667.
7. Kuwajima K. The molten globule state of alpha-lactalbumin. FASEB J 1996;10:102–109.
8. Wu LC, Schulman BA, Peng ZY, Kim PS. Disulfide determinants of calcium-induced packing in alpha-lactalbumin. Biochemistry 1996;35:859–863.
9. Kuwajima K. The molten globule state as a clue for understanding the folding and cooperativity of globular–protein structure. Proteins 1989;6:87–103.
10. Arai M, Kuwajima K. Role of the molten globule state in protein folding. Adv Protein Chem 2000;53:209–282.
11. Lala AK, Kaul P. Increased exposure of hydrophobic surface in molten globule state of alpha-lactalbumin—fluorescence and hydrophobic photolabeling studies. J Biol Chem 1992;267:19914–19918.
12. Gussakovsky EE, Haas E. Two steps in the transition between the native and acid states of bovine alpha-lactalbumin detected by circular polarization of luminescence—evidence for a premolten globule state. Protein Sci 1995;4:2319–2326.
13. Svensson M, Sabharwal H, Hakansson A, Mossberg AK, Lipniunas P, Leffler H, Svanborg C, Linse S. Molecular characterization of alpha-lactalbumin folding variants that induce apoptosis in tumor cells. J Biol Chem 1999;274:6388–6396.
14. Pike ACW, Brew K, Acharya KR. Crystal structures of guinea-pig, goat and bovine alpha-lactalbumin highlight the enhanced conformational flexibility of regions that are significant for its action in lactose synthase. Structure 1996;4:691–703.

15. Grobler JA, Wang M, Pike ACW, Brew K. Study by mutagenesis of the roles of 2 aromatic clusters of alpha-lactalbumin in aspects of its action in the lactose synthase system. J Biol Chem 1994;269: 5106–5114.
16. Joniau M, Pardon E, Maisonneuve JF, Haezebrouck P, Desmet J, Van Dael H, De Baetselier A. Site directed mutants of bovine alpha-lactalbumin with reduced capacity to activate lactose synthesis. In: Geisow MJ, editor. Perspectives on protein engineering (CD ROM, ISBN 0-9529015-0-1). UK: Biodigm; 1996.
17. Malinovskii VA, Tian J, Grobler JA, Brew K. Functional site in alpha-lactalbumin encompasses a region corresponding to a subsite in lysozyme and parts of two adjacent flexible substructures. Biochemistry 1996;35:9710–9715.
18. Greene LH, Grobler JA, Malinovskii VA, Tian J, Acharya KR, Brew K. Stability, activity and flexibility in alpha-lactalbumin. Protein Eng 1999;12:581–587.
19. Ramakrishnan B, Qasba PK. Crystal structure of lactose synthase reveals a large conformational change in its catalytic component, the beta 1,4-galactosyltransferase-I. J Mol Biol 2001;310:205–218.
20. Ramakrishnan B, Shah PS, Qasba PK. alpha-Lactalbumin (LA) stimulates milk beta-1,4-galactosyltransferase I (beta 4GAL-T1) to transfer glucose from UDP-glucose to N-acetylglucosamine–crystal structure of beta 4GAL-T1-LA complex with UDP-Glc. J Biol Chem 2001;276:37665–37671.
21. Clark PL, Liu ZP, Zhang JH, Gierasch LM. Intrinsic tryptophans of crabpi as probes of structure and folding. Protein Sci 1996;5: 1108–1117.
22. Wang WQ, Xu Q, Shan YF, Xu GJ. Probing local conformational changes during equilibrium unfolding of firefly luciferase: fluorescence and circular dichroism studies of single tryptophan mutants. Biochem Biophys Res Commun 2001;282:28–33.
23. Chakraborty S, Ittah V, Bai P, Luo L, Haas E, Peng ZY. Structure and dynamics of the alpha-lactalbumin molten globule: fluorescence studies using proteins containing a single tryptophan residue. Biochemistry 2001;40:7228–7238.
24. Chaudhuri TK, Horii K, Yoda T Arai M, Nagata S, Terada TP, Uchiyama H, Ikura T, Tsumoto K, Kataoka H, Matsushima M, Kuwajima K, Kumagai I. Effect of the extra N-terminal methionine residue on the stability and folding of recombinant alpha-lactalbumin expressed in *Escherichia coli*. J Mol Biol 1999;285:1179–1194.
25. Chaudhuri TK, Arai M, Terada TP, Ikura T, Kuwajima K. Equilibrium and kinetic studies on folding of the authentic and recombinant forms of human alpha-lactalbumin by circular dichroism spectroscopy. Biochemistry 2000;39:15643–15651.
26. Ishikawa N, Chiba T, Chen LT, Shimizu A, Ikeguchi M, Sugai S. Remarkable destabilization of recombinant alpha-lactalbumin by an extraneous N-terminal methionyl residue. Protein Eng 1998;11: 333–335.
27. Noppe W, Haezebrouck P, Hanssens I, De Cuyper M. A simplified purification procedure of alpha-lactalbumin from milk using Ca^{2+}-dependent adsorption in hydrophobic expanded bed chromatography. Bioseparation 1998;8:153–158.
28. Viaene A, Volckaert G, Joniau M, Debaetselier A, Vancauwelaert F. Efficient expression of bovine alpha-lactalbumin in *Saccharomyces cerevisiae*. Eur J Biochem 1991;202:471–477.
29. Pardon E, Haezebrouck P, Debaetselier A, Hooke SD, Fancourt KT, Desmet J, Dobson CM, Van Dael H, Joniau M. A Ca^{2+}-binding chimera of human lysozyme and bovine alpha-lactalbumin that can form a molten globule. J Biol Chem 1995;270:10514–10524.
30. Hinnen A, Hicks JB, Fink GR. Transformation of yeast. Proc Natl Acad Sci USA 1978;75:1929–1933.
31. Laroche Y, Storme V, Demeutter J, Messens J, Lauwereys M. High-level secretion and very efficient isotopic labeling of tick anticoagulant peptide (TAP) expressed in the methylotrophic yeast, *Pichia pastoris*. Bio-Technology 1994;12:1119–1124.
32. Saito A, Usui M, Song Y, Azakami H, and Kato A. Secretion of glycosylated alpha-lactalbumin in yeast *Pichia pastoris*. J Biol Chem 2002;132:77–82.
33. Gill SC, von Hippel PH. Calculation of protein extinction coefficients from amino-acid sequence data. Anal Biochem 1989;182:319–326.
34. Pace CN. Determination of urea and guanidine hydrochloride denaturation curves. Methods Enzymol 1986;4:2411–2423.
35. Brew K, Vanaman TC, Hill RL. The role of alpha-lactalbumin and the A protein in lactose synthetase: a unique mechanism for the control of a biological reaction. Proc Natl Acad Sci USA 1968;59: 491–497.
36. Venyaminov SY, Yang JY. Determination of protein secondary structure. In: Fasman GD, editor. Circular dichroism and the conformational analysis of biomolecules. New York: Plenum Press; 1996. p 69–107.
37. Saeki K, Arai M, Yoda T, Nakao M, Kuwajima K. Localized nature of the transition-state structure in goat alpha-lactalbumin folding. J Mol Biol 2004;341:589–604.
38. Woody RW, Dunker AK. Aromatic and cystine side-chain circular dichroism in proteins. In: Fasman GD, editor. Circular dichroism and the conformational analysis of biomolecules. New York: Plenum Press, 1996. p 109–157.
39. Peng ZY, Kim PS. A protein dissection study of a molten globule. Biochemistry 1994;33:2136–2141.
40. Wu LC, Peng ZY, Kim PS. Bipartite structure of the alpha-lactalbumin molten globule. Nat Struct Biol 1995;2:281–286.
41. Böhm G, Muhr R, Jaenicke R. Quantitative-analysis of protein far UV circular-dichroism spectra by neural networks. Protein Eng 1992;5:191–195.
42. Sommers PB, Kronman MJ. Intermolecular and intramolecular interactions of alpha-lactalbumin—comparative fluorescence properties of bovine, goat, human and guinea-pig alpha-lactalbumin—characterization of the environments of individual tryptophan residues in partially folded conformers. Biophys Chem 1980;11:217–232.
43. Hendrix TM, Griko YV, Privalov PL. Energetics of structural domains in alpha-lactalbumin. Protein Sci 1996;5:923–931.
44. Vanderheeren G, Hanssens I, Meijberg W, Van Aerschot A. thermodynamic characterization of the partially unfolded state of Ca^{2+}-loaded bovine alpha-lactalbumin: evidence that partial unfolding can precede Ca^{2+} release. Biochemistry 1996;35:16753–16759.
45. Hendrix T, Griko YV, Privalov PL. A calorimetric study of the influence of calcium on the stability of bovine alpha-lactalbumin. Biophys Chem 2000;84:27–34.
46. Vanhooren A, Vanhee K, Noyelle K, Majer Z, Joniau M, Hanssens I. Structural basis for difference in heat capacity increments for Ca^{2+} binding to two alpha-lactalbumins. Biophys J 2002;82:407–417.
47. Eftink MR. Use of fluorescence spectroscopy as thermodynamics tool. Methods Enzymol 2000;323:459–473.
48. Vanhooren A, Devreese B, Vanhee K, Van Beeumen J, Hanssens I. Photoexcitation of tryptophan groups induces reduction of two disulfide bonds in goat alpha-lactalbumin. Biochemistry 2002;41: 11035–11043.
49. Harata K, Muraki M. X-ray structural evidence for a local helix-loop transition in alpha-lactalbumin. J Biol Chem 1992;267: 1419–1421.
50. Chedad A, Van Dael H. Kinetics of the folding and unfolding of goat alpha-lactalbumin. Proteins 2004;57:345–356.
51. Veprintsev DB, Permyakov SE, Permyakov EA, Rogov VV, Cawthern KM, Berliner LJ. Cooperative thermal transitions of bovine and human apo-alpha-lactalbumins: evidence for a new intermediate state. FEBS Lett 1997;412:625–628.
52. Markovic-Housley Z, Stolz B, Lanz R, Erni B. Effect of tryptophan to phenylalanine substitutions on the structure, stability and enzyme activity of the IIAB subunit of the mannose transporter of *Esherichia coli*. 1999;8:1530–1535.
53. Kuwajima K, Mitani M, Sugai S. Characterization of the critical state in protein folding—effects of guanidine-hydrochloride and specific Ca^{2+} binding on the folding kinetics of alpha-lactalbumin. J Mol Biol 1989;206:547–5461.
54. Matouschek A, Kellis JT, Serrano L, Fersht AR. Mapping the transition-state and pathway of protein folding by protein engineering. Nature 1989;340:122–126.
55. Serrano L, Matouschek A, Fersht AR. The folding of an enzyme. 3. Structure of the transition-state for unfolding of barnase analyzed by a protein engineering procedure. J Mol Biol 1992;224:805–818.
56. Ikeguchi M, Fujino M, Kato M, Kuwajima K, Sugai S. Transition state in the folding of alpha-lactalbumin probed by the 6-120 disulfide bond. Protein Sci 1998;7:1564–1574.
57. Schulman BA, Redfield C, Peng ZY, Dobson CM, and Kim PS. Different subdomains are most protected from hydrogen-exchange in the molten globule and native states of human alpha-lactalbumin. J Mol Biol 1995;253:651–657.
58. Demarest SJ, Boice JA, Fairman R, Raleigh DP. Defining the core structure of the alpha-lactalbumin molten globule state. J Mol Biol 1999;294:213–221.
59. Guex N, Peitsch MC. Swiss-model and the Swiss-PDB viewer: an environment for comparative protein modeling. Electrophoresis 1997;18:2714–2723.